Frontiers in Bioscience Landmark

Front. Biosci. (Landmark Ed) **2026**; 31(4): 47702
https://doi.org/10.31083/FBL47702

Original Research

Effect of Endogenous FGF21 Deficiency on the Inflammatory Microenvironment of the Retina

Ting-ting Zhao[1,2,†], Ming-kai Chang[3,†], Bai-yun Shen[2], Hao-ran Guo[3], Yu-tong Han[3], Wen-fei Wang[2,3,*]

[1]Department of Ophthalmology, Aier Eye Hospital, Jinan University, 510071 Guangzhou, Guangdong, China
[2]Department of Fundus Diseases, Nanning Aier Eye Hospital, 530000 Nanning, Guangxi, China
[3]School of Life Science, Northeast Agricultural University, 150030 Harbin, Heilongjiang, China
*Correspondence: wangwenfei@neau.edu.cn (Wen-fei Wang)
[†]These authors contributed equally.

Academic Editors: Dario Rusciano and Gabriella Lupo
Submitted: 26 October 2025 Revised: 10 February 2026 Accepted: 13 March 2026 Published: 27 April 2026

Abstract

Background: While the systemic metabolic role of fibroblast growth factor 21 (FGF21) is well-established, its function in retinal homeostasis and its link to retinal diseases like age-related macular degeneration (AMD) and diabetic retinopathy (DR) remains poorly understood. This study investigated the impact of endogenous FGF21 deficiency on the retinal immune microenvironment. **Methods**: Retinal structure was assessed in FGF21 KO and wild-type mice using spectral-domain optical coherence tomography. Transcriptomic profiles of the retina/choroid were analyzed by RNA-seq. Differentially expressed genes (DEGs) were identified (DESeq2, FDR <0.05), clustered, and interrogated by Kyoto Encyclopedia of Genes and Genomes (KEGG) pathway enrichment. Immune-cell composition was inferred with ImmuCellAI. **Results**: FGF21 KO mice showed no overt retinal structural defects under baseline conditions. Nevertheless, 449 DEGs were identified (293 up, 156 down in knockout). Pathway analysis revealed significant enrichment of cytokine–cytokine receptor interaction, chemokine signaling, and Jak-STAT cascades. Immune deconvolution indicated a significant increase in M2-polarised macrophages ($p < 0.01$) without change in total macrophage number. Expression of key inflammatory mediators including Il1b was concordantly altered. **Conclusions**: This work establishes endogenous FGF21 as a crucial local immunomodulator and defines a novel mechanistic link to retinal disease susceptibility, supporting its further exploration as a therapeutic target.

Keywords: FGF21; retina; RNA-Seq; macrophages; immunomodulation

1. Introduction

The retina is essential for vision, and its dysfunction is a major cause of irreversible blindness worldwide. With aging populations, the prevalence of sight-threatening retinal diseases such as diabetic retinopathy (DR) and age-related macular degeneration (AMD) has risen markedly, representing a critical public health challenge [1]. Understanding the pathogenesis of these conditions and developing effective interventions are therefore central goals in ophthalmology research.

Fibroblast Growth Factor 21 (FGF21) is a hepatokine with systemic metabolic regulatory functions [2]. Previous studies have demonstrated its pivotal role in modulating glycolipid metabolism [3], exerting antioxidant [4] and anti-inflammatory [5], and attenuating the aging process [6]. Intriguingly, recent studies suggest that exogenous FGF21 administration may protect against various retinal pathologies, including DR and dry AMD [7–11], implying a potential role in maintaining retinal health. However, the mechanisms underlying these protective effects, and particularly the physiological function of endogenous FGF21 in the retina, remain poorly understood.

To elucidate the functional mechanism underlying FGF21's protective role in retinal homeostasis, the FGF21 knockout mice were used to investigate whether endogenous FGF21 influences retinal homeostasis. We first assessed retinal structure *in vivo* and then performed transcriptomic analysis of retinal/choroidal tissues to identify molecular changes caused by FGF21 deficiency. Our results reveal that loss of endogenous FGF21 disrupts retinal immune homeostasis, notably by shifting macrophage polarization toward an M2-dominant phenotype, thereby rendering the retina more susceptible to injury. These findings establish endogenous FGF21 as a key local immunomodulator and provide a mechanistic foundation for exploring its therapeutic potential in retinal diseases.

2. Materials and Methods

2.1 Animal Experiments

All animal experiments conducted in this study were approved in advance by Northeast Agricultural University. FGF21 knockout mice (FGF21 KO mice, KO group) were purchased from Cyagen Biosciences Inc. (Suzhou, Contract No. KOAIP180401WZ1+KOAIP180401WZ2). C57BL/6 mice of equivalent age (WT group) were ob-

tained from Liaoning Chang Sheng Biotechnology Co., Ltd. (Liaoning, China). All animals were housed in a controlled environment with a 12-hour light/12-hour dark cycle, provided with ad libitum access to food and water, and shielded from external stimuli. The ambient temperature for housing was maintained at 22 ± 2 ℃. A total of 36 female mice were used in this study. Prior to the OCT imaging, mice were anesthetized with Avertin (1.25% w/v solution, 30 µL/g, MA0478, Dalian Meilun Biotechnology Co., Ltd, Dalian, Liaoning, China). At the end of the experiment, all animals were humanely euthanized. Euthanasia was performed by cervical dislocation under deep anesthesia (induced by the same Avertin solution (1.25% w/v, 30 µL/g, i.p.) used for OCT imaging). The absence of a pedal reflex was confirmed to ensure death before any tissue collection. Then the retinal/choroidal tissues were harvested for RNA-seq and other analyses.

To determine whether endogenous FGF21 deficiency affects retinal resilience under pathological stress, mice were allocated into two independent disease-modeling experiments (n = 6 per genotype per model). For diabetic retinopathy (DR) Model, because of the hypersensitivity of FGF21 KO mice to streptozotocin (STZ) (HY-13753, MedChemExpress, Shanghai, China), diabetes was induced using genotype-specific protocols. WT mice received intraperitoneal injections of STZ (30 mg/kg/day for 5 consecutive days) while maintained on a high-fat diet (HFD, 1135DM). FGF21 KO mice were fed the same HFD without STZ injection until their fasting blood glucose levels exceeded 11.1 mmol/L. Diabetic mice (fasting glucose >11.1 mmol/L from both groups) were maintained for an additional 8 weeks before analysis. For dry Age-related Macular Degeneration (dAMD) Model, both FGF21 KO and WT mice were allowed to freely consume drinking water containing 0.8% hydroquinone for three months to induce oxidative retinal damage. Optical coherence tomography (OCT) was performed at the endpoint of each model to assess retinal structural integrity (n = 6).

To investigate the direct effect of endogenous FGF21 deletion on retinal homeostasis in the absence of external stressors, a separate cohort of mice (n = 6 per genotype, WT and FGF21 KO) was examined at 6 weeks of age under normal physiological conditions. After baseline OCT imaging, mice were euthanized, and neural retina/choroid complexes were promptly harvested. Tissues from each group were pooled for bulk RNA sequencing (n = 3 mice), and other mice per group were used for subsequent qPCR validation (n = 3 retina/choroid complexes) and immunohistochemistry (n = 3 retina/choroid complexes).

2.2 Immunohistochemistry

Eyeballs were fixed with 4% paraformaldehyde, dehydrated, cleared, and embedded in paraffin. Sections (4–5 µm) were dewaxed and subjected to heat-induced epitope retrieval (HIER). After blocking endogenous peroxidase activity with 3% H_2O_2 and nonspecific sites with 10% horse serum, sections were incubated with primary antibodies against CD163 (bs2527R, 1:100, Bioss, Beijing, China). Following PBS washes, sections were incubated with a Goat Anti-Rabbit IgG H&L antibody (bs-0295G-HRP, 1:200, Bioss, Beijing, China), developed with 3,3-diaminobenzidine (DAB) (HY-W014212, MedChemExpress, Shanghai, China), and counterstained with hematoxylin (C0107, Beyotime, Shanghai, China).

For semi-quantification of CD163 staining, whole-section images were analyzed using ImageJ software (NIH, Bethesda, USA) with the "IHC Toolbox" plugin. The integrated optical density (IOD) of the DAB (brown) signal, which reflects the amount of CD163 protein within the tissue, was measured in a defined region of the entire retinal section.

2.3 Oral Glucose Tolerance Test (OGTT)

Following a 12-h fast, mice were weighed and baseline blood glucose was measured prior to oral gavage of glucose (2 g/kg). Blood glucose levels were then monitored at 30-minute intervals for 120 minutes. Glucose tolerance was determined by calculating the area under the curve (AUC) for blood glucose over time using Origin 2021 (OriginLab Corporation, Northampton, MA, USA) software.

2.4 Optical Coherence Tomography (OCT) Imaging

Mice were anesthetized via intraperitoneal Avertin (1.25% w/v solution, 30 µL/g, MA0478, Dalian Meilun Biotechnology Co., Ltd, Dalian, Liaoning, China). Pupillary dilation was achieved using tropicamide-phenylephrine eye drops (1–2 drops per eye, Santen Pharmaceutical Co., Ltd, Suzhou, Jiangsu, China). Throughout the procedure, ophthalmic hydroxypropyl methylcellulose (UV-Gel) (Shanghai Haohai Biological Technology Co., Ltd., Shanghai, China) was intermittently applied to the eyes of the mice to safeguard the cornea. OCT images were captured using the VG200D imaging camera system (SVision imaging, Ltd, San Jose, CA, USA).

2.5 RNA Seq

RNA-Seq testing was commissioned to the Biotechnology Company (Shanghai, China).

2.6 Real-Time PCR (qPCR)

Total RNA was extracted from tissues using the TRIzol reagent (Invitrogen Life Technologies, Carlsbad, CA, USA). Then, the first-strand cDNA was synthesized using a HiScript II 1st Strand cDNA Synthesis Kit (R212-01, Vazyme, Nanjing, Jiangsu, China). The gene expression was detected with a Taq Pro Universal SYBR qPCR Master Mix Kit (Q712-02, Vazyme, Nanjing, Jiangsu, China), according to the manufacturer's protocol. The expression for each gene was calculated using the expression $2^{-\triangle\triangle Ct}$

Table 1. Primer sequences for qPCR.

Gene	Forward primer	Reverse primer
Tnf	GCCACCACGCTCTTCTGTCTACT	TGGTTTGTGAGTGTGAGGGTCTGG
Il1b	ATCTCGCAGCAGCACATCAACAAG	GGTCCACGGGAAAGACACAGGTAG
Pparg	TCGCCAAGGTGCTCCAGAAGATG	GGTGAAGGCTCATGTCTGTCTCTGT
Ccl5	ACTCCCTGCTGCTTTGCCTACC	TTGGCGGTTCCTTCGAGTGACAA
Cxcl1	ATGGCTGGGATTCACCTCAAGAACA	GAGTGTGGCTATGACTTCGGTTTGG
Ptgs2	AACACCTGAGCGGTTACCACTTCAA	AGGCAATGCGGTTCTGATACTGGAA
Lep	GGTTCCTGTGGCTTTGGTCCTATCT	GGATACCGACTGCGTGTGTGAAATG
Adipoq	GCCTGGAGAAGCCGCTTATGTGTA	ACTTGCCAGTGCTGCCGTCAT
Fos	GCCAGTCAAGAGCATCAGCAACG	AGGAACCGGACAGGTCCACATCT
Retn	TCTTCCTTGTCCCTGAACTGCTGG	GCTCAAGACTGCTGTGCCTTCTG
CD163	GGTTCTTCTTGGAGGTGCTGGATCT	CCGCCAGTCTCAGTTCCTTCTTCA
CD206/MRC	ACCTGGCAAGTATCCACAGCATTGA	GCAGTCCTCCTGTCTGTTGTTCTCA

method. The Real-time PCR primers used in this study were synthesized by Sangon Biotech (Shanghai) Co., Ltd. The primer sequences are shown in Table 1.

2.7 Differential Expression Analysis and Disease-Related Gene Acquisition

DESeq was employed for the analysis, with the screening criteria set as p value < 0.05 and a multiplicity of difference $|\log2\text{FoldChange}| > 1$ to identify significantly different genes. The results of the expression difference analysis were visualized using BioLadder (https://www.bioladder.cn). Disease-related gene sets were retrieved from three public databases: GeneCards (https://www.genecards.org), DisGeNET (https://www.disgenet.org), and the Therapeutic Target Database (TTD, https://db.idrblab.net/ttd).

2.8 Construction of a Protein-Protein Interaction (PPI) Network

The relevant genes obtained from the screening were imported into the STRING website (http://string-db.org) to construct the protein-protein interaction (PPI) network [12]. The results of the PPI network were then visualized and enhanced using Cytoscape (version 3.10.0, https://cytoscape.org, National Resource for Network Biology, USA). To comprehensively analyze the PPI network and identify key components, the cytoHubba [13] plugin was utilized. Specifically, the Maximal Clique Centrality (MCC) algorithm was employed to screen for key genes, facilitating the construction of sub-networks and identification of pivotal components within the PPI network.

2.9 Functional Enrichment Analysis

The analysis was carried out by using R software (v.4.2.2) package clusterProfiler (v.4.5.0) [14] through Hiplot Pro (https://hiplot.com.cn/), a comprehensive web service for biomedical data analysis and visualization.

2.10 Correlation Analysis

The correlation coefficients between the variables were computed through Pearson correlation analysis. A grid plot was generated to display the genes in the group with an absolute correlation coefficient greater than 0.8 and a p-value less than 0.05. This facilitated the visualization of interactions between significantly correlated feature nodes, aiding in the identification of relationships between the variables. The process of calculation and plotting was conducted using CNSknowall (https://cnsknowall.com/).

2.11 Immunoinfiltration Analysis

Immune Cell Abundance Identifier (ImmuCellAI) is a tool to accurately estimate immune cell abundance from gene expression datasets, including RNA-Seq [15]. In the present study, the Immune Cell Abundance Identifier for mouse (ImmuCellAI-mouse) [16] is used to estimate the abundance of 36 immune cell (sub) types in mouse retina/choroid RNA-Seq data.

2.12 Statistical Analysis

Data are presented as the mean $\pm$ standard error of the mean (SEM). The sample size (n) for each experiment represents biological replicates. Statistical comparisons between two groups were performed using an unpaired, two-tailed Student's t-test. For comparisons among multiple groups, one-way analysis of variance (ANOVA) followed by appropriate post-hoc tests was used. A $p < 0.05$ was considered statistically significant.

3. Results

3.1 FGF21 Deficiency Does not Alter Retinal Structure or Systemic Metabolism Under Baseline Conditions

To assess the intrinsic role of endogenous FGF21, we first examined retinal structure and systemic metabolism in unchallenged, 6-week-old mice. *In vivo* spectral-domain optical coherence tomography (OCT) revealed comparable retinal thickness, reflectivity, and overall architecture between wild-type (WT) and FGF21 knockout (KO) mice

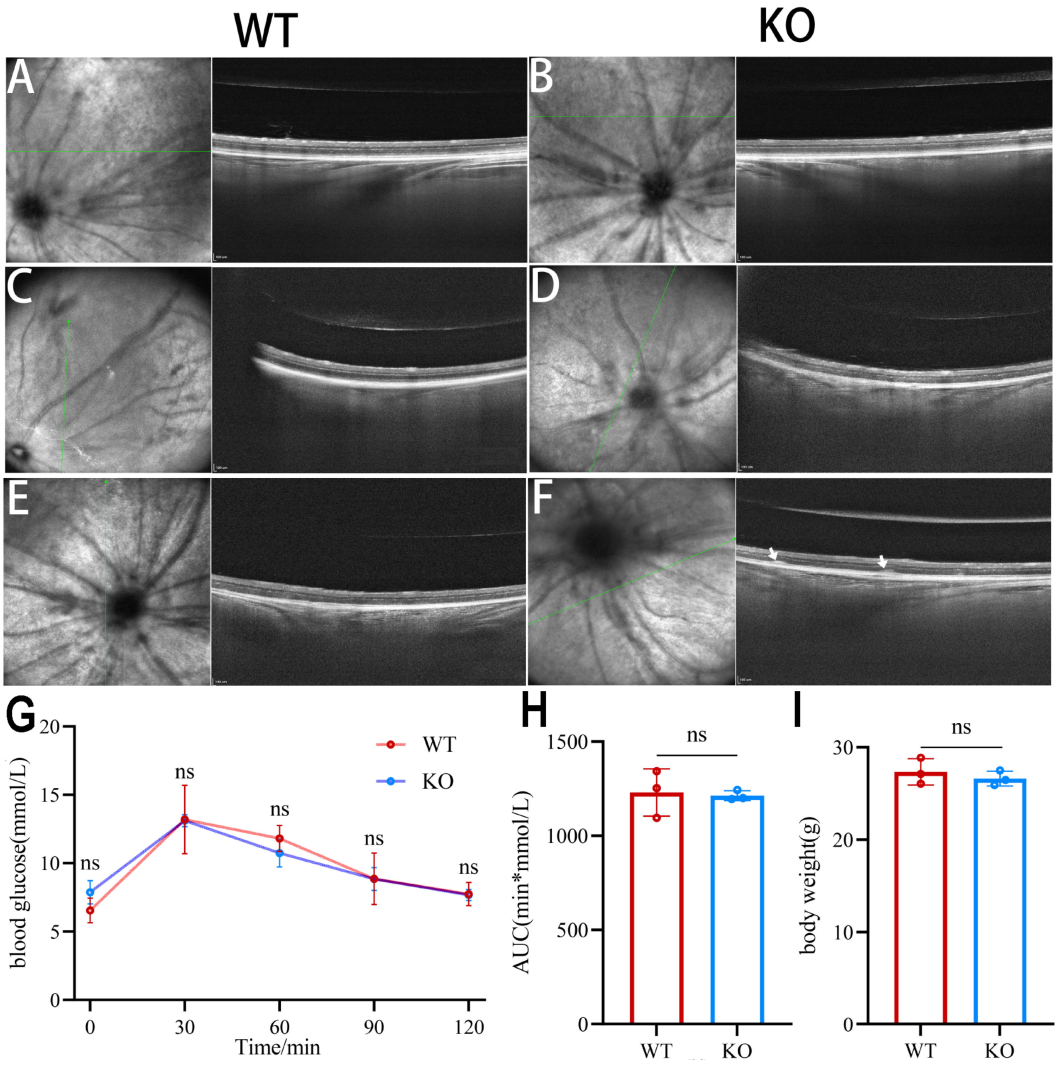

Fig. 1. Fibroblast Growth Factor 21 (FGF21) knockout exacerbates retinal structural damage induced by hyperglycemia and oxidative stress in mouse models. (A–F) OCT detection results of the fundus of mice. (A) 6-week-old WT mice. (B) 6-week-old FGF21 KO mice. (C) WT diabetic mice. (D) FGF21 KO diabetic mice. (E) WT AMD mice. (F) FGF21 KO AMD mice. Green lines indicate the position of the OCT scan line. White arrows indicate drusen, the typical lesions of dry age-related macular degeneration. (G) Oral glucose tolerance test (OGTT) performed in 6-week-old FGF21 KO and WT mice. (H) Area under the curve (AUC) of blood glucose during the OGTT. (I) Body weight measurements of 6-week-old FGF21 KO and WT mice. KO: FGF21 knockout; WT: normal control; ns: $p > 0.05$.

(Fig. 1A,B). Furthermore, FGF21 KO mice showed no significant differences in body weight, fasting blood glucose, or glucose tolerance compared to WT littermates (all $p > 0.05$; Fig. 1G–I).

3.2 FGF21 Deficiency Exacerbates Retinal Structural Damage Under Metabolic or Oxidative Stress

We next investigated whether the absence of FGF21 affects retinal resilience to pathological insults. Quantitative analysis of retinal layer thickness by OCT revealed that FGF21 KO mice exhibited significantly exacerbated structural damage under both pathological conditions.

When subjected to diabetic conditions or hydroquinone-induced oxidative stress (a model for dry age-related macular degeneration), FGF21 KO mice exhibited significantly more severe retinal structural damage than their WT counterparts, as quantified by OCT (Fig. 1C–F). Retinal thickness measurements were performed on the averaged image from three consecutive scans. Using the segmented line tool, three perpendicular measurements were taken from the internal limiting membrane (ILM) to the retinal pigment epithelium (RPE) to determine the total retinal thickness. The values were then averaged to yield a single thickness value per eye.

Under diabetic conditions, the total retinal thickness in FGF21 KO mice was thinner than in WT controls ($p < 0.05$). Similarly, in the hydroquinone-induced AMD model, FGF21 KO mice exhibited more severe thin-

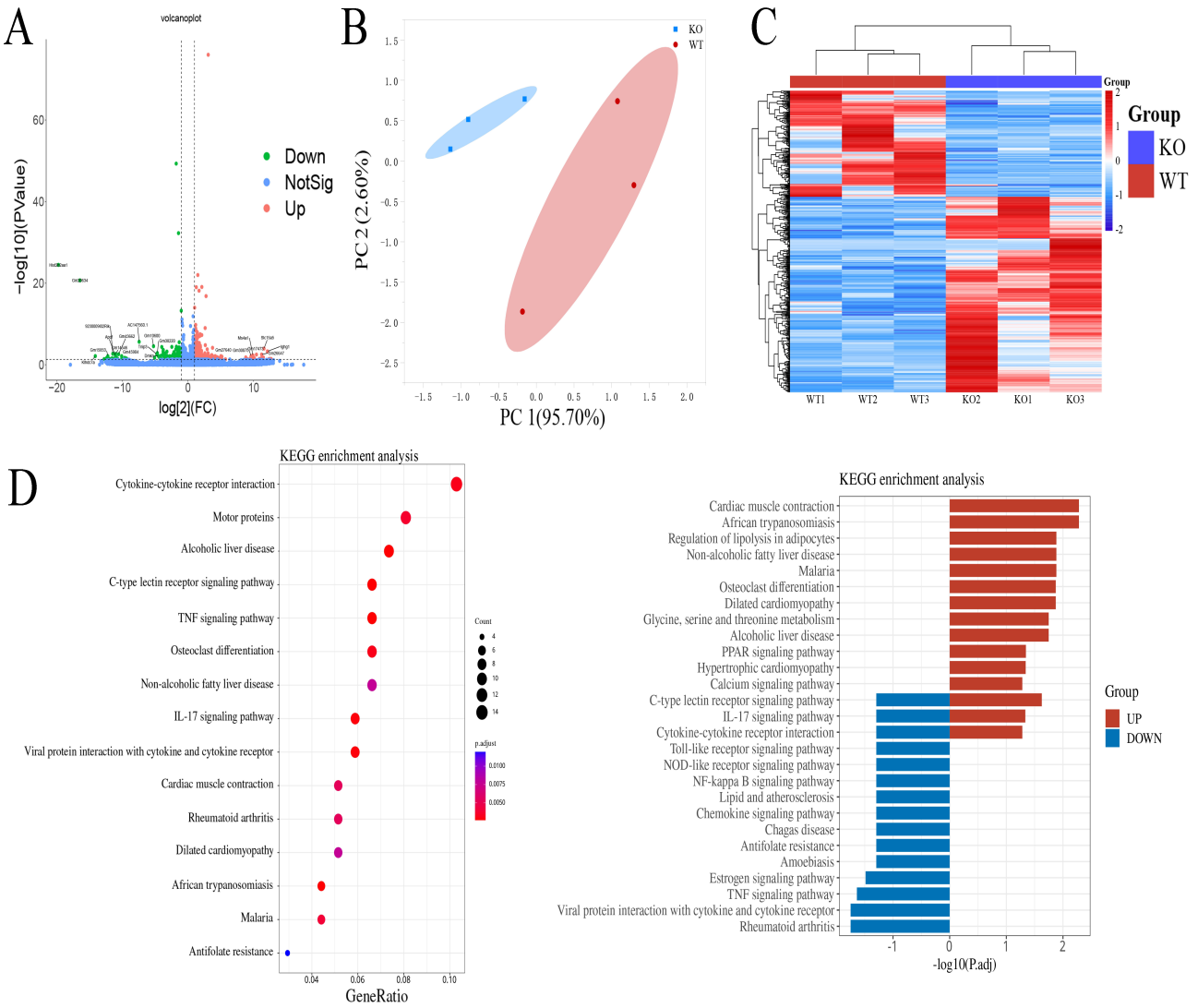

Fig. 2. Transcriptomic profiling reveals differential gene expression patterns in the retina/choroid of FGF21 KO mice compared to WT controls. (A) Volcano plot illustrating differentially expressed genes (DEGs) between KO and WT groups. Significantly up-regulated genes are highlighted in red, while significantly down-regulated genes are shown in green. Blue dots represent non-significantly expressed genes. (B) Principal component analysis (PCA) plot demonstrating the clustering pattern of samples based on the global transcriptome profiles, with PC1 and PC2 indicating the first and second principal components, respectively. (C) Hierarchical clustering heatmap of differentially expressed mRNA. Rows represent individual genes, and columns represent individual samples. Color scale indicates normalized expression levels, with red denoting high expression and blue denoting low expression. (D) Kyoto Encyclopedia of Genes and Genomes (KEGG) pathway enrichment analysis of DEGs. KO: FGF21 knockout; WT: normal control.

ning (**Supplementary Fig. 1**). In addition to thickness, OCT analysis revealed discrete hyperreflective foci and irregularities in the Bruch membrane area of FGF21 KO mice, suggestive of drusen-like deposits (white arrow). These results indicate that endogenous FGF21 is crucial for maintaining retinal homeostasis, and its deficiency predisposes the tissue to injury under stress.

3.3 FGF21 Deficiency Alters the Retinal/Choroidal Transcriptomic Profile

Transcriptomic analysis of retinal/choroidal complexes from 6-week-old FGF21 KO and WT mice revealed 449 differentially expressed genes (DEGs) ($p < 0.05$, $|\log2FoldChange| > 1$), with 293 up-regulated and 156 down-regulated in the KO group (Fig. 2A). Principal component analysis (PCA) demonstrated a clear separation between the genotypes along the first principal component (PC1, 95.7% of variance), indicating a fundamental shift in the global transcriptional landscape upon FGF21 deficiency (Fig. 2B). Unsupervised hierarchical clustering heatmaps of the DEGs also distinctly segregated the WT and KO samples (Fig. 2C).

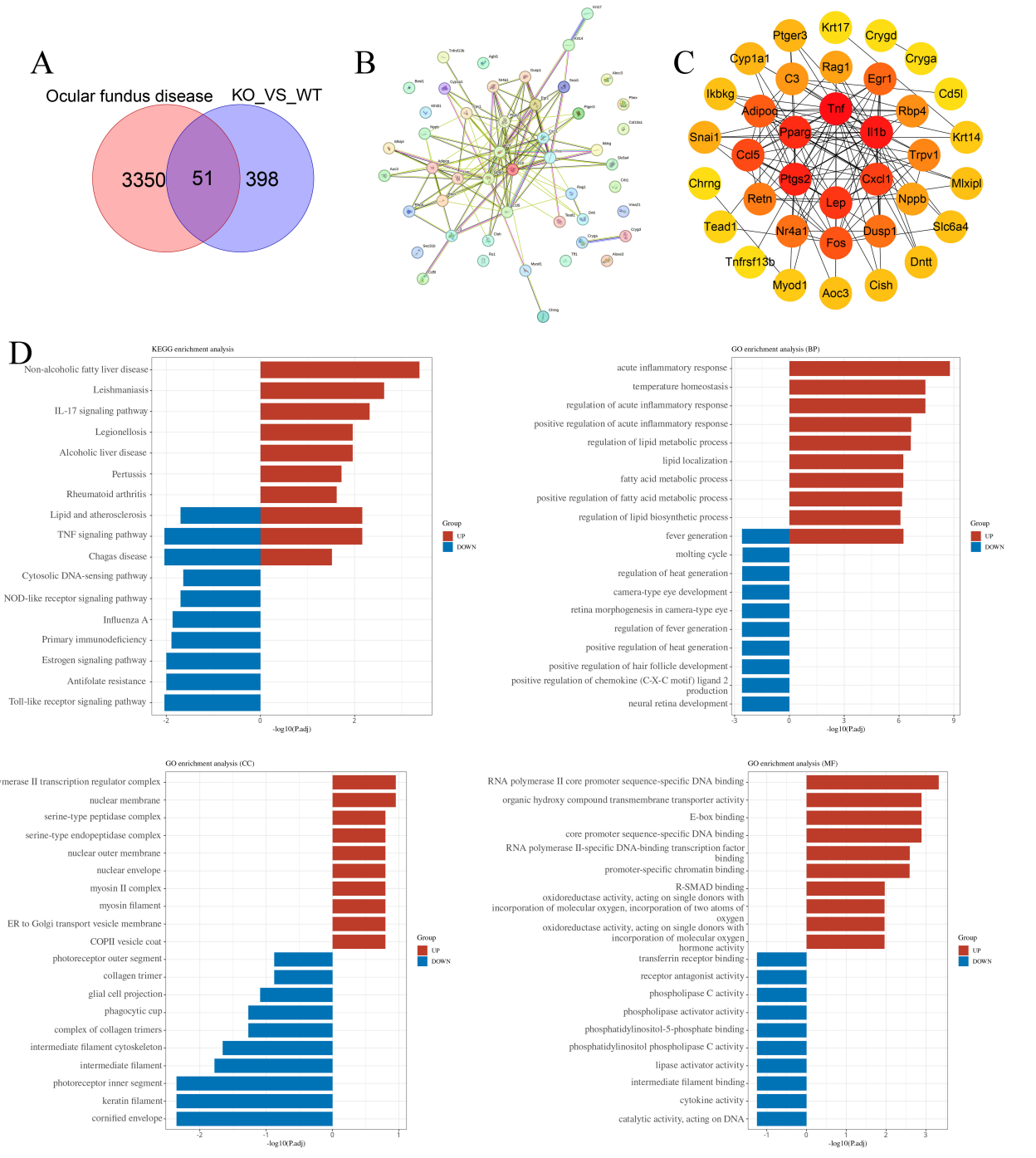

Fig. 3. Integration analysis identifies FGF21 deficiency-associated retinal/choroidal differentially expressed genes (DEGs) overlapping with ocular fundus disease signature genes and their functional interaction networks. (A) Venn diagram depicting the intersection between retinal/choroidal DEGs from FGF21 KO mice and ocular fundus disease-associated genes curated from the GeneCards database. (B) PPI network diagram. Nodes represent individual proteins, and edges indicate predicted functional interactions. (C) Identification of hub genes from the PPI network using the Maximal Clique Centrality (MCC) algorithm implemented in CytoHubba plugin of Cytoscape. The top-ranked core genes are displayed in descending order of MCC scores, with color intensity proportional to the centrality ranking. (D) KEGG versus GO enrichment analysis. KO: FGF21 knockout; WT: normal control.

Kyoto Encyclopedia of Genes and Genomes (KEGG) pathway enrichment analysis of these DEGs highlighted significant involvement in immune and inflammatory pathways. The most enriched terms included Cytokine-cytokine receptor interaction signaling pathway, Motor proteins, Alcoholic liver disease, C-type lectin receptor signaling pathway, and TNF signaling pathway (Fig. 2D).

3.4 Correlation Analysis Between FGF21 Deficiency-Induced DEGs and Ocular Fundus Disease Related Genes

To explore the disease relevance of the transcriptomic changes, we intersected the 449 DEGs with known fundus disease-associated genes from the GeneCards database (relevance score >1; 3401 genes). This yielded 51 overlapping genes (Fig. 3A). A protein-protein interaction (PPI) network constructed from these 51 genes using the STRING database (species: Mus musculus) revealed significant interconnectivity (Fig. 3B). Further analysis of this network in Cytoscape using the Maximal Clique Centrality (MCC) algorithm identified six hub genes: tumor necrosis factor (Tnf), interleukin 1β (Il1b), prostaglandin-endoperoxide synthase 2 (Ptgs2), peroxisome proliferator-activated receptor γ (Pparg), leptin (Lep), and C-X-C motif chemokine 1 (Cxcl1) (Fig. 3C). The MCC algorithm scores for these genes were 14,711, 14,574, 13,752, 13,138, 11,658, and 11,526, respectively.

Functional enrichment analysis of these hub genes highlighted their involvement in key pathways and biological processes. KEGG pathway analysis showed enrichment in the TNF signaling pathway, Non-alcoholic fatty liver disease, and Leishmaniasis. Gene Ontology (GO) analysis indicated associations with the Acute inflammatory response, Temperature homeostasis, Photoreceptor inner segment, Keratin filament, Cornified envelope, RNA polymerase II core promoter sequence-specific DNA binding (Fig. 3D).

3.5 Intersection Analysis of FGF 21 KO-Induced Retinal/Choroidal Differential Genes With AMD/DR-Related Genes

To delineate the specific relevance of FGF21 deficiency to age-related macular degeneration (AMD) and diabetic retinopathy (DR), we intersected our DEG list with disease-associated genes from GeneCards, DisGeNET, and Therapeutic Target Database. After applying a relevance score filter (>10 for GeneCards), 33 genes were common to the FGF21 KO DEGs and the combined AMD/DR gene sets (Fig. 4A).

Pearson correlation analysis between these 33 candidate genes and members of the FGF19 subfamily (including FGF21) and their receptors (FGFRs) revealed several significant associations: Mlxipl and Aoc3 showed strong positive correlations with FGFR1, Fos, Retn, and Adipoq correlated positively with FGFR4, and Fos also correlated with FGF15. In contrast, Cd5l exhibited a strong negative correlation with Fgf23 (Fig. 4B–D). Functional enrichment analysis of these 33 overlapping genes highlighted acute inflammatory response as a key biological process linking the FGF21-deficient retinal phenotype to both AMD and DR pathogenesis (Fig. 5A,B).

In addition, we constructed a PPI network from these genes using STRING and Cytoscape, which comprised 27 nodes and 109 interactionsFunctional enrichment analysis of these 33 overlapping genes (Fig. 5D). Application of the MCC algorithm identified five central hub genes: tumor necrosis factor (Tnf), interleukin 1β (Il1b), peroxisome proliferator-activated receptor γ (Pparg), chemokine (Ccl5), and C-X-C motif chemokine 1 (Cxcl1) (Fig. 5E,F). Notably, Pparg, Il1b, and Cxcl1 were upregulated in FGF21 KO mice, while Tnf and Ccl5 were downregulated. The alterations in gene transcription were further validated through qPCR (Fig. 5C).

3.6 Immunoinfiltration Analysis

To investigate the effect of FGF21 deficiency on the immune microenvironment, we estimated immune cell abundances from the RNA-seq data using the ImmuCellAI-mouse. The results revealed a significant shift in immune cell composition in FGF21 KO retinal/choroidal tissues. Specifically, the abundance of M2 macrophages was markedly increased, whereas NKT cells and germinal center B cells were decreased compared to WT controls (Fig. 6A,B).

Subsequently, Pearson correlation analysis between the abundance of these altered immune cells and key DEGs (Tnf, Il1b, Pparg, Ccl5, Cxcl1) showed a clear dichotomy. The increased M2 macrophage signature positively correlated with Il1b, Pparg, and Cxcl1, but negatively correlated with Tnf and Ccl5. The opposite correlation pattern was observed for the diminished NKT and Germinal center B cell populations (Fig. 6C). Together, these data indicate that FGF21 deficiency dramatically alters the retinal immune milieu, primarily by disrupting macrophage homeostasis.

4. Discussion

Exogenous administration of fibroblast growth factor 21 (FGF21) or its analogs has shown therapeutic promise in animal models of various retinal disorders, including diabetic retinopathy, retinitis pigmentosa and retinal neovascularization [7–10]. Our prior work further demonstrated its protective effect against the progression of dry age-related macular degeneration (dAMD) [11]. These consistent findings across models underscore FGF21 signaling as a potential therapeutic target for retinal diseases.

However, a critical gap exists between the well-characterized pharmacological effects of FGF21 and the understanding of its endogenous physiological functions. Notably, whereas administration of recombinant FGF21 improves systemic metabolism (reducing hyperglycemia and body weight) [17–20], FGF21 KO or its coreceptor β-klotho often present with complex, and sometimes paradoxical, metabolic phenotypes under different conditions [21–23]. This discrepancy underscores the context-dependent complexity of FGF21 biology and highlights that the consequences of chronic endogenous deficiency cannot be simply extrapolated from acute exogenous supplementation. Thus, elucidating the specific role of endogenous FGF21 in retinal

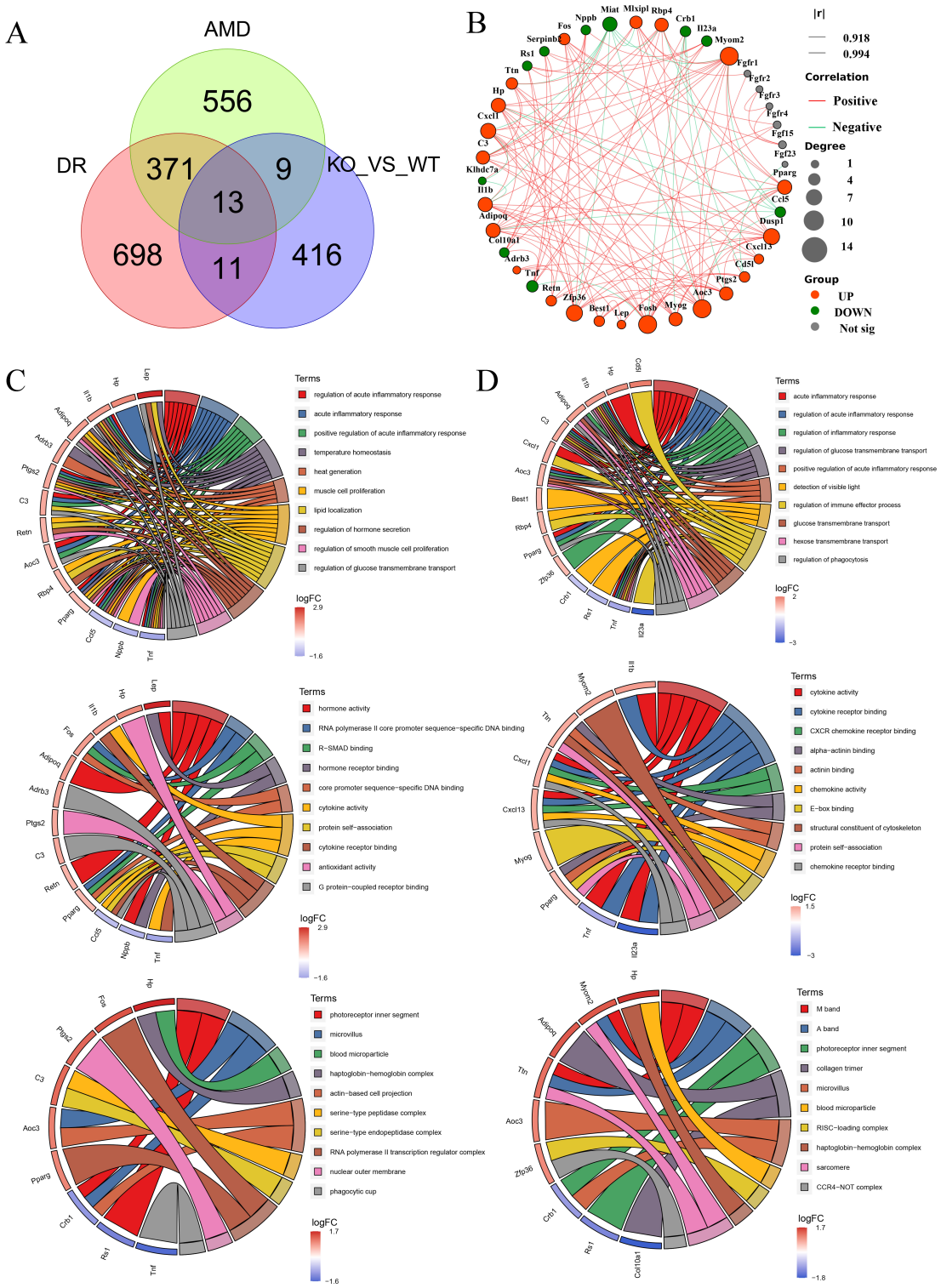

Fig. 4. Gene enrichment analysis of age-related macular degeneration (AMD)/diabetic retinopathy (DR) associated DEGs between KO and WT groups. (A) Venn diagrams depicting DR and AMD-related genes with significantly different genes from three databases: GeneCards, DisGeNET, and Therapeutic Target Database. (B) Correlation between disease (AMD and DR) related genes, FGF receptors, and FGF19 subfamily members. (C) Chord plot illustrating GO enrichment analysis of DR-related differential genes. (D) Chord plot illustrating GO enrichment analysis of AMD-associated differential genes. Differential genes are presented on the left, with color changes indicating alterations in log2FC from small to large, with red indicating up-regulated and blue indicating down-regulated genes. Enrichment term results are displayed on the right, and the two are linked to indicate gene enrichment into that term. KO: FGF21 knockout; WT: normal control.

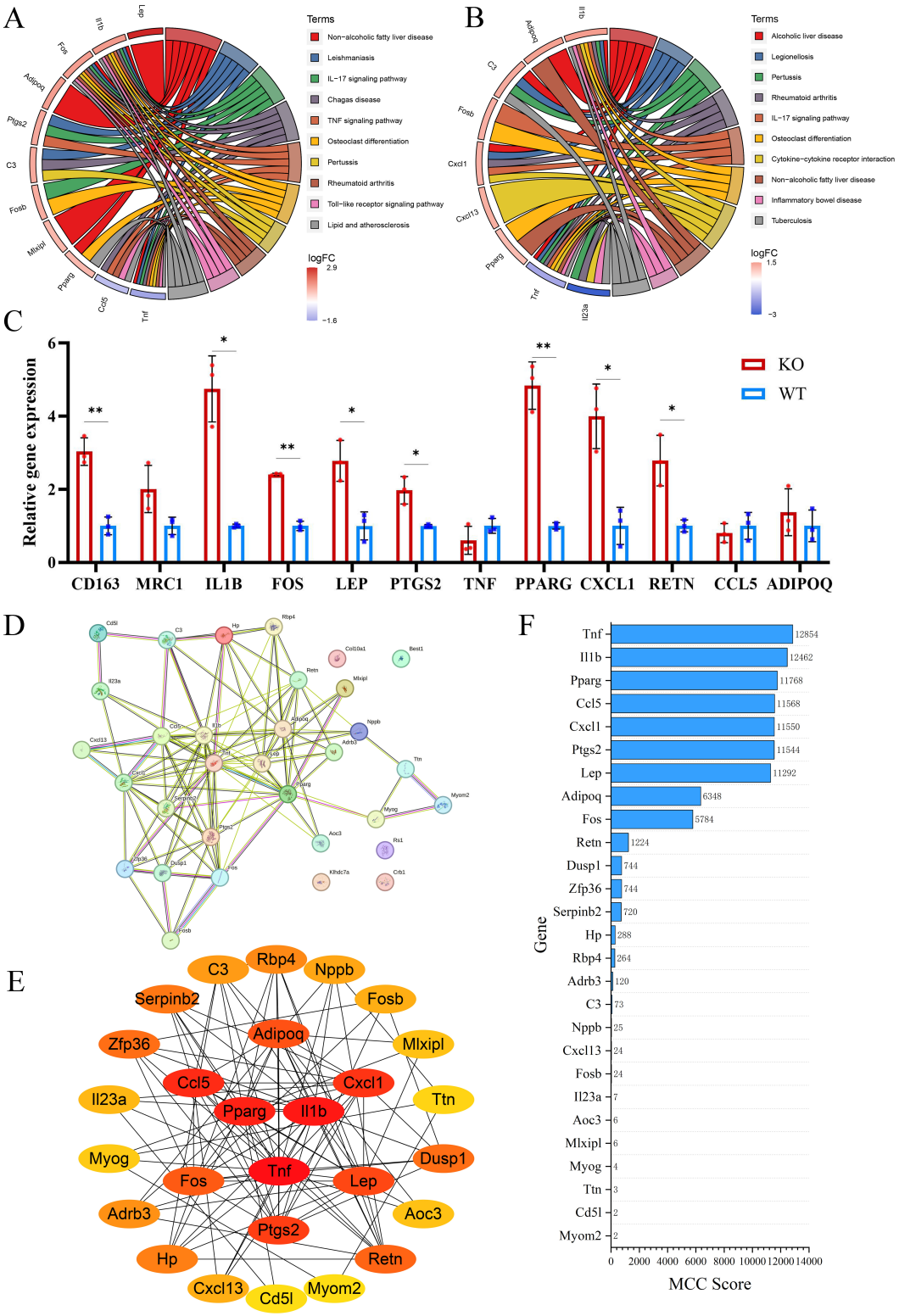

Fig. 5. Screening of core DEGs related to AMD/DR in the retina/chorioid of FGF21 KO mice. (A) STRING diagram illustrating KEGG enrichment analysis of DR-related differential genes. (B) STRING diagram illustrating KEGG enrichment analysis of AMD-related differential genes. On the left side are the differential genes, with color changes indicating the change in log2FC from small to large, where red represents up-regulation and blue represents down-regulation. On the right side are the enrichment term results, and the two are connected to indicate gene enrichment into that term. (C) Real-time PCR analysis for differential genes in indicated groups. (D) PPI network diagram. (E) Core differential genes identified by the MCC algorithm. (F) MCC scores and rankings of related genes. KO: FGF21 knockout; WT: normal control. Statistical significance is indicated as * $p < 0.05$ and ** $p < 0.01$.

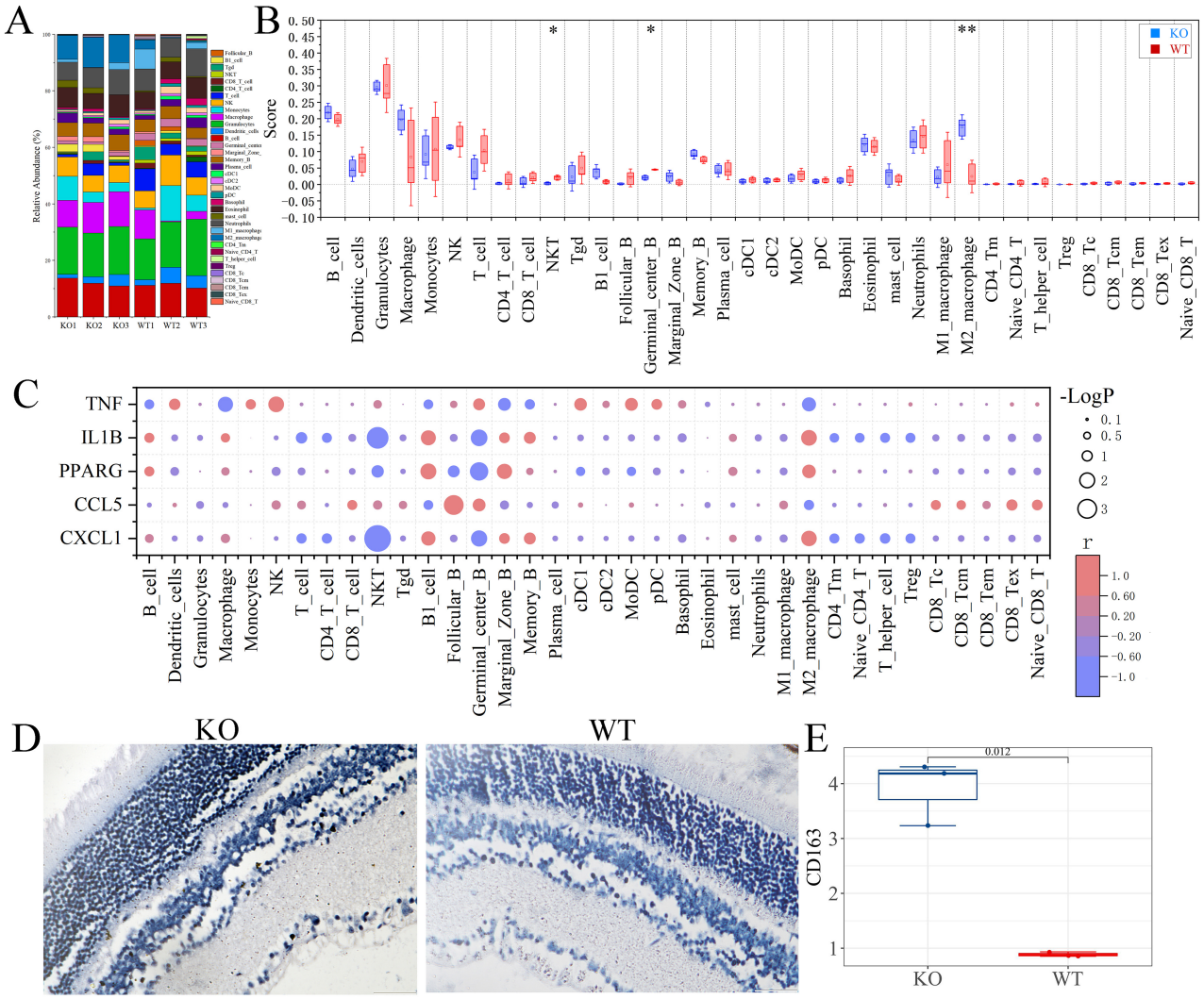

Fig. 6. Immune infiltration analysis. (A) Relative percentages of 36 infiltrating immune cells in the KO group versus the WT group. (B) Box plot of 36 infiltrating immune cells in the KO group versus the WT group. (C) Bubble plots showing the correlation between differential genes and immune cells. Bubble colors represent the magnitude of correlation coefficients, indicating positive and negative correlations. The size of the bubbles represents the magnitude of the *p*-value, signifying the significance level of this sample. (D) Representative images of IHC staining for CD163. (E) Quantification of CD163 staining. Scale bar = 50 µm. *, $p < 0.05$; **, $p < 0.01$. KO: FGF21 knockout; WT: normal control.

homeostasis and its relevance to retinal disease pathogenesis is critical for its translational development.

Importantly, while exogenous FGF21 alleviates retinal pathology, overt structural lesions are rarely reported in unchallenged FGF21 KO mice. In line with this, our study also found no detectable fundus abnormalities in 6-week-old KO mice. The results indicate that endogenous FGF21 is not required for maintaining gross retinal structure under physiological conditions.

However, transcriptomic analysis revealed a contrasting picture at the molecular level. Despite the absence of structural or systemic metabolic defects, FGF21 deficiency significantly altered multiple inflammatory and metabolic pathways within the retinal/choroidal tissue. The lack of concurrent systemic metabolic dysregulation in our mice allows us to attribute these transcriptional changes primarily to the local absence of FGF21 signaling in the retina/choroid, rather than secondary effects of whole-body metabolic disturbance.

The disease relevance of these transcriptomic alterations was underscored by the significant overlap between our DEGs and genes associated with major retinal diseases, particularly AMD and DR. Among the intersecting genes, key regulators of inflammation and immunity emerged, including Il1b, Cxcl1, and Pparg (upregulated), as well as Tnf and Ccl5 (downregulated). This signature strongly indicates that FGF21 deficiency fundamentally reshapes the retinal inflammatory microenvironment.

Retinal inflammation is a pivotal driver in the pathogenesis of AMD and DR [24–26]. This study reveals that endogenous FGF21 deficiency creates a complex immune milieu distinct from the anti-inflammatory effects of its pharmacological supplementation. This complexity is exemplified by two observations: first, the downregulation of Tnf in KO mice, contrasting with reports that exogenous FGF21 can reduce TNF-α in disease models [7], and second, the positive correlation at the tissue level between the M2 marker CD163 and the pro-inflammatory mediators IL-1β and CXCL1.

The first paradox likely originates from the fundamental difference between chronic genetic deficiency and acute pharmacological intervention. The former permits long-term adaptations, such as the marked compensatory upregulation of Pparg we observed. Given that PPARγ is a potent transcriptional repressor of the NF-κB pathway (a primary driver of Tnf expression) [27,28], the Tnf downregulation may be secondary to sustained PPARγ activation. This interpretation is reinforced by our parallel discovery of an increased proportion of cells with an M2-like phenotype, a cell state often associated with PPAR γ activity [29].

The second observation can be understood by looking beyond the classical M1/M2 dichotomy. Recent studies emphasize that macrophage activation exists on a functional continuum, where specific subsets can produce pro-inflammatory factors including IL-1β while expressing markers like CD163, adapting to specific tissue contexts [30]. Therefore, FGF21 deficiency likely induces a unique immune microenvironment. Within this milieu, the accumulation of M2-like macrophages coexists with pro-inflammatory signals derived from various cellular sources (including activated glia and endothelial cells) [31,32], together establishing a pathological foundation that predisposes the retina to injury.

Thus, the immune microenvironment in the retina of FGF21 KO mice appears to be reconfigured rather than simply attenuated. The concurrent rise in Il1b suggests a shift towards a specific inflammatory axis, while the PPARγ-mediated suppression of Tnf may reflect a counter-regulatory mechanism. This phenomenon underscores that the role of endogenous FGF21 in retinal homeostasis is to maintain a balanced immune environment. Critically, this altered landscape is characterized by a co-dominance of pro-inflammatory signals and the accumulation of M2-like macrophages, as evidenced by bioinformatic inference of cell abundance and the confirmed increase in CD163+ cells density.

Additionally, the observed shift toward an M2-like macrophages underscores a disruption in macrophage polarization homeostasis, a critical aspect of retinal immune balance. Given the high plasticity of macrophages, this M2-skewed state in young FGF21 KO mice may represent a specific adaptation to the early, FGF21-deficient microenvironment. It is plausible that this balance could shift further under prolonged stress or with aging. Regardless of the specific phenotype, the overall increase in macrophage presence and the imbalance itself are recognized as key drivers of retinal pathology. Both M1 and M2 macrophages can contribute to pathogenic processes such as abnormal neovascularization through distinct mechanisms, thereby promoting the progression of diseases like AMD and DR [33–35]. Thus, the dysregulated macrophage landscape we identified provides a plausible cellular mechanism linking endogenous FGF21 deficiency to increased retinal disease susceptibility.

5. Conclusion

While our study in FGF21 KO mice establishes a principled link between endogenous FGF21 and retinal immune homeostasis, several considerations must be addressed when translating these findings to human disease. First, inherent species differences in retinal anatomy and immune cell repertoire may modulate the phenotype. Second, human age-related macular degeneration (AMD) and diabetic retinopathy (DR) are multifactorial, chronic disorders influenced by genetics, environment, and aging. In contrast, this study uses a single-gene knockout model raised in a controlled, simplified laboratory environment, which cannot fully replicate the multifaceted nature of the human conditions. Nonetheless, our discovery provides a testable hypothesis for human pathology. Future studies should prioritize: (1) validating this immune signature in human retinal sections or vitreous samples from AMD/DR patients, correlating FGF21 pathway activity with macrophage polarization markers; (2) employing human retinal organoids or induced pluripotent stem cell (iPSC)-derived microglia/macrophage co-cultures to dissect the cell-autonomous effects of FGF21 signaling in a human genetic background; and (3) exploring targeted therapeutic strategies, such as developing eye-localized delivery systems for FGF21 analogs or modulators of its downstream targets (PPARγ etc.), to circumvent systemic metabolic effects and directly address retinal immune dysregulation. Collectively, this work provides a foundational immune framework, positioning FGF21 not merely as a metabolic hormone but as a local gatekeeper of retinal immune balance, whose therapeutic manipulation warrants careful, context-specific investigation.

5. Limitations

This study also has several limitations. First, as an exploratory investigation, the sample size for the transcriptomic analysis, though aligned with similar discovery-phase studies, may limit the detection of genes with subtle expression changes. Nevertheless, the robust pathways and cell population shifts we identified provide strong preliminary evidence and clear targets for future hypothesis-driven studies with appropriate power analysis.

Second, while we have provided protein-level validation for the central immunological phenotype (M2 macrophage increase via CD163 IHC, Fig. 6D,E) and transcriptional validation for key cytokines, we acknowledge that we did not perform comprehensive protein quantification for all identified differentially expressed genes (DEGs). This was primarily due to the limited protein yield from mouse retinal/choroidal tissues. Our validation strategy was therefore intentionally focused on confirming the most robust and functionally central finding. Finally, while our data reveal a strong association between the M2-skewed microenvironment and increased disease susceptibility. Direct functional assays, such as macrophage-specific depletion or adoptive transfer experiments, are required to establish causality. Future work should prioritize such functional validation alongside the proteomic and spatial transcriptomic approaches noted above.

Availability of Data and Materials

The raw data supporting the conclusions of this article will be made available by the authors on request.

Author Contributions

Conceptualization, TZ and BS; Methodology, MC and HG; Software, MC; Investigation, TZ, MC, WW, HG; Formal analysis, BS, MC; Validation, YH; Data curation, TZ, WW, MC; Writing—original draft preparation, TZ and MC; Writing—review and editing, WW; Supervision, BS, WW. All authors have read and agreed to the final version of the manuscript. All authors contributed to editorial changes in the manuscript. All authors have participated sufficiently in the work and agreed to be accountable for all aspects of the work.

Ethics Approval and Consent to Participate

The study was conducted in accordance with the ARRIVE guidelines (https://arriveguidelines.org) and was approved by the Animal Ethics Committee of Northeast Agricultural University (NEAUEC20240135).

Acknowledgment

We give our sincere thanks to Grace Liu, Oliver Kang and Lismarie Sun from Intalight company for their help in this study.

Funding

This research was funded by grants from the Guangxi Natural Science Foundation Project, China (2025GXNSFAA069182); Natural Science Foundation of Hunan Province, China (2023JJ70050); Guangxi Zhuang Autonomous Region Health Commission Self-funded Scientific Research Project (Z-A20251080).

Conflicts of Interest

The authors declare no conflicts of interest. No funding or employment was received from Intalight company.

Declaration of AI and AI-Assisted Technologies in the Writing Process

In this study, to enhance the linguistic quality of the paper, we employed an artificial intelligence language polishing tool, ChatGPT, to optimize certain paragraphs. We chose to use this tool due to its outstanding performance in terms of language fluency and grammatical accuracy. We ensured that all polishing work was carried out without altering the original research data and analysis results. The specific polishing process involved a section-by-section assessment of the initial draft, followed by modifications based on the tool's suggestions. We believe that this method of polishing has improved the readability and professionalism of the paper while maintaining the integrity and accuracy of the research content. After using this tool, the authors reviewed and edited the content as needed and takes full responsibility for the content of the publication.

Supplementary Material

Supplementary material associated with this article can be found, in the online version, at https://doi.org/10.31083/FBL47702.

References

[1] Wong WL, Su X, Li X, Cheung CMG, Klein R, Cheng CY, *et al*. Global prevalence of age-related macular degeneration and disease burden projection for 2020 and 2040: a systematic review and meta-analysis. The Lancet. Global Health. 2014; 2: e106–e116. https://doi.org/10.1016/S2214-109X(13)70145-1.

[2] Prida E, Álvarez-Delgado S, Pérez-Lois R, Soto-Tielas M, Estany-Gestal A, Fernø J, *et al*. Liver Brain Interactions: Focus on FGF21 a Systematic Review. International Journal of Molecular Sciences. 2022; 23: 13318. https://doi.org/10.3390/ijms232113318.

[3] Nauck MA, Wefers J, Meier JJ. Treatment of type 2 diabetes: challenges, hopes, and anticipated successes. The Lancet. Diabetes & Endocrinology. 2021; 9: 525–544. https://doi.org/10.1016/S2213-8587(21)00113-3.

[4] Kang K, Xu P, Wang M, Chunyu J, Sun X, Ren G, *et al*. FGF21 attenuates neurodegeneration through modulating neuroinflammation and oxidant-stress. Biomedicine & Pharmacotherapy = Biomedecine & Pharmacotherapie. 2020; 129: 110439. https://doi.org/10.1016/j.biopha.2020.110439.

[5] Li JY, Wang N, Khoso MH, Shen CB, Guo MZ, Pang XX, *et al*. FGF-21 Elevated IL-10 Production to Correct LPS-Induced Inflammation. Inflammation. 2018; 41: 751–759. https://doi.org/10.1007/s10753-018-0729-3.

[6] Youm YH, Horvath TL, Mangelsdorf DJ, Kliewer SA, Dixit VD. Prolongevity hormone FGF21 protects against immune senescence by delaying age-related thymic involution. Proceedings of the National Academy of Sciences of the United States of America. 2016; 113: 1026–1031. https://doi.org/10.1073/pnas.1514511113.

[7] Fu Z, Gong Y, Liegl R, Wang Z, Liu CH, Meng SS, *et al*. FGF21 Administration Suppresses Retinal and Choroidal Neo-

vascularization in Mice. Cell Reports. 2017; 18: 1606–1613. https://doi.org/10.1016/j.celrep.2017.01.014.

[8] Fu Z, Lundgren P, Pivodic A, Yagi H, Harman JC, Yang J, *et al*. FGF21 via mitochondrial lipid oxidation promotes physiological vascularization in a mouse model of Phase I ROP. Angiogenesis. 2023; 26: 409–421. https://doi.org/10.1007/s10456-023-09872-x.

[9] Fu Z, Wang Z, Liu CH, Gong Y, Cakir B, Liegl R, *et al*. Fibroblast Growth Factor 21 Protects Photoreceptor Function in Type 1 Diabetic Mice. Diabetes. 2018; 67: 974–985. https://doi.org/10.2337/db17-0830.

[10] Tomita Y, Fu Z, Wang Z, Cakir B, Cho SS, Britton W, *et al*. Long-Acting FGF21 Inhibits Retinal Vascular Leakage in In Vivo and In Vitro Models. International Journal of Molecular Sciences. 2020; 21: 1188. https://doi.org/10.3390/ijms21041188.

[11] Zhao T, Wang W, Gao K, Li S, Jiang Y, Yang Z, *et al*. Fibroblast growth factor-21 alleviates phenotypic characteristics of dry age-related macular degeneration in mice. Experimental Eye Research. 2022; 218: 109014. https://doi.org/10.1016/j.exer.2022.109014.

[12] Szklarczyk D, Gable AL, Lyon D, Junge A, Wyder S, Huerta-Cepas J, *et al*. STRING v11: protein-protein association networks with increased coverage, supporting functional discovery in genome-wide experimental datasets. Nucleic Acids Research. 2019; 47: D607–D613. https://doi.org/10.1093/nar/gky1131.

[13] Chin CH, Chen SH, Wu HH, Ho CW, Ko MT, Lin CY. cytoHubba: identifying hub objects and sub-networks from complex interactome. BMC Systems Biology. 2014; 8 Suppl 4: S11. https://doi.org/10.1186/1752-0509-8-S4-S11.

[14] Wu T, Hu E, Xu S, Chen M, Guo P, Dai Z, *et al*. clusterProfiler 4.0: A universal enrichment tool for interpreting omics data. Innovation (Cambridge (Mass.)). 2021; 2: 100141. https://doi.org/10.1016/j.xinn.2021.100141.

[15] Miao YR, Zhang Q, Lei Q, Luo M, Xie GY, Wang H, *et al*. ImmuCellAI: A Unique Method for Comprehensive T-Cell Subsets Abundance Prediction and its Application in Cancer Immunotherapy. Advanced Science (Weinheim, Baden-Wurttemberg, Germany). 2020; 7: 1902880. https://doi.org/10.1002/advs.201902880.

[16] Miao YR, Xia M, Luo M, Luo T, Yang M, Guo AY. ImmuCellAI-mouse: a tool for comprehensive prediction of mouse immune cell abundance and immune microenvironment depiction. Bioinformatics (Oxford, England). 2022; 38: 785–791. https://doi.org/10.1093/bioinformatics/btab711.

[17] Geng L, Lam KSL, Xu A. The therapeutic potential of FGF21 in metabolic diseases: from bench to clinic. Nature Reviews. Endocrinology. 2020; 16: 654–667. https://doi.org/10.1038/s41574-020-0386-0.

[18] Tan H, Yue T, Chen Z, Wu W, Xu S, Weng J. Targeting FGF21 in cardiovascular and metabolic diseases: from mechanism to medicine. International Journal of Biological Sciences. 2023; 19: 66–88. https://doi.org/10.7150/ijbs.73936.

[19] Coskun T, Bina HA, Schneider MA, Dunbar JD, Hu CC, Chen Y, *et al*. Fibroblast growth factor 21 corrects obesity in mice. Endocrinology. 2008; 149: 6018–6027. https://doi.org/10.1210/en.2008-0816.

[20] Xu J, Lloyd DJ, Hale C, Stanislaus S, Chen M, Sivits G, *et al*. Fibroblast growth factor 21 reverses hepatic steatosis, increases energy expenditure, and improves insulin sensitivity in diet-induced obese mice. Diabetes. 2009; 58: 250–259. https://doi.org/10.2337/db08-0392.

[21] Geng L, Liao B, Jin L, Huang Z, Triggle CR, Ding H, *et al*. Exercise Alleviates Obesity-Induced Metabolic Dysfunction via Enhancing FGF21 Sensitivity in Adipose Tissues. Cell Reports. 2019; 26: 2738–2752.e4. https://doi.org/10.1016/j.celrep.2019.02.014.

[22] Hotta Y, Nakamura H, Konishi M, Murata Y, Takagi H, Matsumura S, *et al*. Fibroblast growth factor 21 regulates lipolysis in white adipose tissue but is not required for ketogenesis and triglyceride clearance in liver. Endocrinology. 2009; 150: 4625–4633. https://doi.org/10.1210/en.2009-0119.

[23] Liang Q, Zhong L, Zhang J, Wang Y, Bornstein SR, Triggle CR, *et al*. FGF21 maintains glucose homeostasis by mediating the cross talk between liver and brain during prolonged fasting. Diabetes. 2014; 63: 4064–4075. https://doi.org/10.2337/db14-0541.

[24] Biasella F, Plössl K, Baird PN, Weber BHF. The extracellular microenvironment in immune dysregulation and inflammation in retinal disorders. Frontiers in Immunology. 2023; 14: 1147037. https://doi.org/10.3389/fimmu.2023.1147037.

[25] Murakami Y, Ishikawa K, Nakao S, Sonoda KH. Innate immune response in retinal homeostasis and inflammatory disorders. Progress in Retinal and Eye Research. 2020; 74: 100778. https://doi.org/10.1016/j.preteyeres.2019.100778.

[26] Perez VL, Caspi RR. Immune mechanisms in inflammatory and degenerative eye disease. Trends in Immunology. 2015; 36: 354–363. https://doi.org/10.1016/j.it.2015.04.003.

[27] Chen Y, Zhang X, Yang L, Li M, Li B, Wang W, *et al*. Decreased PPAR-γ expression in the conjunctiva and increased expression of TNF-α and IL-1β in the conjunctiva and tear fluid of dry eye mice. Molecular Medicine Reports. 2014; 9: 2015–2023. https://doi.org/10.3892/mmr.2014.2041.

[28] Mukohda M, Stump M, Ketsawatsomkron P, Hu C, Quelle FW, Sigmund CD. Endothelial PPAR-γ provides vascular protection from IL-1β-induced oxidative stress. American Journal of Physiology. Heart and Circulatory Physiology. 2016; 310: H39–H48. https://doi.org/10.1152/ajpheart.00490.2015.

[29] Abdalla HB, Napimoga MH, Lopes AH, de Macedo Maganin AG, Cunha TM, Van Dyke TE, *et al*. Activation of PPAR-γ induces macrophage polarization and reduces neutrophil migration mediated by heme oxygenase 1. International Immunopharmacology. 2020; 84: 106565. https://doi.org/10.1016/j.intimp.2020.106565.

[30] Jarosova R, Ondrackova P, Leva L, Nedbalcova K, Vicenova M, Masek J, *et al*. Cytokine expression by CD163+ monocytes in healthy and Actinobacillus pleuropneumoniae-infected pigs. Research in Veterinary Science. 2022; 152: 1–9. https://doi.org/10.1016/j.rvsc.2022.07.015.

[31] Padovani-Claudio DA, Morales MS, Smith TE, Ontko CD, Namburu NS, Palmer SA, *et al*. Induction, amplification, and propagation of diabetic retinopathy-associated inflammatory cytokines between human retinal microvascular endothelial and Müller cells and in the mouse retina. Cellular Signalling. 2024; 124: 111454. https://doi.org/10.1016/j.cellsig.2024.111454.

[32] Garcia MJ, Beall AL, Morales MS, Beatty NJ, Palmer SA, Jhala M, *et al*. IL-8 receptor signaling as a novel target for angiogenic retinopathies. Angiogenesis. 2025; 29: 2. https://doi.org/10.1007/s10456-025-10015-7.

[33] Gao S, Li C, Zhu Y, Wang Y, Sui A, Zhong Y, *et al*. PEDF mediates pathological neovascularization by regulating macrophage recruitment and polarization in the mouse model of oxygen-induced retinopathy. Scientific Reports. 2017; 7: 42846. https://doi.org/10.1038/srep42846.

[34] Yang Y, Liu F, Tang M, Yuan M, Hu A, Zhan Z, *et al*. Macrophage polarization in experimental and clinical choroidal neovascularization. Scientific Reports. 2016; 6: 30933. https://doi.org/10.1038/srep30933.

[35] Zhu Y, Zhang L, Lu Q, Gao Y, Cai Y, Sui A, *et al*. Identification of different macrophage subpopulations with distinct activities in a mouse model of oxygen-induced retinopathy. International Journal of Molecular Medicine. 2017; 40: 281–292. https://doi.org/10.3892/ijmm.2017.3022.